

Photoluminescence and Electroluminescence of Carbazole-based Conjugated Dendritic Molecules

Min Ju Cho^a, Young Min Kim^{**b}, Byeong-Kwon Ju^{*b}, and Dong Hoon Choi^{*a}

Abstract

A novel class of conjugated dendritic molecules bearing N-hexyl-substituted carbazoles as peripheral groups and various conjugative aromatic cores was synthesized through Heck coupling and the Horner-Emmons reaction. A multilayered structure of ITO/PEDOT:PSS (30 nm)/emitting material (50 nm)/BCP (10 nm)/Alq₃ (10 nm)/LiF (1 nm)/Al (100 nm) was employed to evaluate the synthesized dendritic materials.

The electroluminescence spectrum of the multilayered device made of 3Cz predominantly exhibited blue emissions. Similar emissions were observed in the PL spectra of its the device's thin film. The multilayered devices made of 3Cz, 3BCz, and 4BCz showed luminance values of 6,250 cd m⁻² at 24 V, 3,000 cd m⁻² at 25 V, and 1,970 cd m⁻² at 36 V, respectively. The smallest molecule, 3Cz, which bore three carbazole peripheral groups, exhibited a blue-like emission with CIE 1931 chromaticity coordinates of $x = 0.17$ and $y = 0.21$.

Keywords: dendritic molecule, absorption, photoluminescence, electroluminescence, blue emission

1. Introduction

Recently, semiconducting organic materials have attracted considerable interest as suitable candidate materials in the fields of electronics and optoelectronics [1–3]. Among the many applications of these organic materials, electroluminescent (EL) devices that use organic materials with a low molar mass are the most popular and have already been employed in practical applications such as flat-panel or flexible display devices [4–9].

The use of functional dendrimers has been proposed for the preparation of multi-chromophoric material systems that possess unique molecular architectures and characteristics. They may be employed for charge transportation and also as luminescent materials in light-emitting devices (LEDs) [10–14]. It has been found that the photophysical properties of the dendritic core, such as the absorption and

emission behaviors, can be fine-tuned by modifying the environment around the core [15–16].

Efficient hole carrier transport is a prerequisite for achieving high-performance EL devices accompanied by well-balanced hole injection and electron injection. In a multilayer device, the individual layers should be optimized to arrive at the most suitable highest occupied molecular orbital (HOMO) and lowest unoccupied molecular orbital (LUMO) energy levels. By fine-tuning these energy levels, many promising hole-transporting layer (HTL) materials in a multilayer device have been suggested to enhance hole injection and block electrons. Thus, confined excitons have been formed in the emitting layer (EML) [17–18].

The use of functional multi-branched molecules has been proposed for the fabrication of the functional layer in EL devices, since their molecular architecture is unique and they possess characteristics that optimize the proper HOMO and LUMO energy levels. They can be easily synthesized so that they would be free from impurities that can behave as carrier traps. They can also be employed as carrier-transporting materials and as luminescent-host materials in EL devices [19]. Carbazole derivatives have been well adopted in the design of hole-transport molecules or host molecules in light-harvesting material systems. Recently, J. Y. Li et. al. reported the interesting properties of carbazole-

Manuscript received August, 8; accepted for publication September, 26
This work was supported financially by LG Display Under its Grant M1-0302-00-0027 (2008). Prof. D. H. Choi of the Seoul R&BD Program provided additional financial support (2008–2009).

Corresponding Author: Dong Hoon Choi

* Member, KIDS; ** Student Member, KIDS

^aDepartment of Chemistry, College of Science, Korea University, 5 Anam, Sungbuk, Seoul 136-701, Korea

^bDisplay and Nanosystem Laboratory, College of Engineering, Korea University, 5 Anam, Sungbuk, Seoul 136-701, Korea

E-mail : dhchoi8803@korea.ac.kr Tel : 02-3290-3140 Fax : 02-924-3141

based multi-branched molecules [20-21]. 1,3,5-Tris[2-(9-ethylcarbazyl-3)ethylene]benzene (TECEB) was prepared as a hole-transporting material for organic light-emitting devices (OLEDs). They claimed that it is comparable to 1,4-bis(1-naphthyl phenylamino)biphenyl (NPB) in terms of their HOMO/LUMO energy levels and carrier drift mobility. Although it was suggested as superior to NPB in terms of its higher glass-transition temperature ($T_g = 130^\circ\text{C}$) and ease of synthesis, it was found unsuitable in the wet processing of the multilayer EL device. It should be evaporated to form a hole-transporting layer under a high vacuum.

The photophysical properties of a novel class of conjugated dendritic molecules that bear carbazoles as peripheral groups and three conjugative aromatic cores are reported in this paper. Electroluminescence (EL) devices were fabricated using only the new carbazole-based molecules, which displayed good self-film-forming properties. Highly homogeneous and structureless PL and EL spectral behaviors of these molecules were obtained. The 3Cz molecules showed particularly promising EL properties. The density effects of the carbazole moiety at the periphery on the PL and EL characteristics were also investigated. These effects are discussed in this paper with references to possible mechanisms.

2. Experiments

Instrumental analysis

The thermal properties were studied under a nitrogen atmosphere with a Mettler DSC 821^e instrument. A thermal gravimetric analysis (TGA) was conducted with a Mettler TGA50 thermal analysis system under a heating rate of $10^\circ\text{C}/\text{min}$. The redox properties of the synthesized compounds were examined via cyclic voltammetry (Model: EA161 eDAQ). A platinum plate was coated with thin films using chloroform as a solvent. The electrolyte solution used was 0.10M tetrabutylammonium hexafluorophosphate (Bu_4NPF_6) in freshly dried acetonitrile. The Ag/AgCl and Pt wire (0.5 mm in diameter) electrodes were utilized as the reference and counter electrodes, respectively. The scan rate was $50 \text{ mV}/\text{s}$.

Absorption and photoluminescence spectroscopy

To study the absorption and PL spectral behavior, thin films of dendritic molecules were fabricated on quartz substrates as follows. The solution (2.5 wt%) of each molecule

in monochlorobenzene was filtered through an acrodisc syringe filter (Millipore $0.2 \mu\text{m}$) and subsequently spin-cast on the quartz glass. The films were dried overnight at 60°C for 48 hours under a vacuum. The absorption spectra of the film samples and the chloroform solution (conc. 4.0×10^{-6} mole/L) were obtained using a UV-vis spectrometer (HP 8453, PDA type) in the wavelength range of 190–1,100 nm. The PL spectra were recorded with an AMINCO-Bowman Series 2 luminescence spectrometer.

Electroluminescence measurement

The multilayer diode had a structure of ITO/PEDOT:PSS (30 nm)/emitting material (50 nm)/BCP (10 nm)/Alq₃ (10 nm)/LiF (1 nm)/Al (100 nm). The conducting PEDOT layer was spin-coated onto the ITO-coated glasses in an argon atmosphere. The emitting layer was then spin-coated onto the thoroughly dried PEDOT layer using the monochlorobenzene solution (conc: 5 wt%).

For the multilayer devices, the 2,9-dimethyl-4,7-diphenyl-1,10-phenanthroline (BCP) and tris(8-hydroxyquinoline) aluminium (Alq₃) layers were vacuum-deposited using a VPC-260 (ULVAC, Japan) vacuum coater and a CRTM-6000 thickness monitor (ULVAC, Japan) onto the emitting dendrimer layer. Finally, the LiF (1 nm)/Al (100 nm) electrodes were deposited onto the Alq₃ layer under the same conditions.

The EL spectra of the synthesized compounds were also acquired with an AMINCO-Bowman Series 2 luminescence spectrometer. The J-V-L characteristics were measured using an assembly that consisted of DC power supply (Hewlett-Packard 6633B) and a digital multimeter (Hewlett-Packard 34970A). The luminance was measured using a Minolta LS-100 luminance meter. The thickness of the emitting layer was determined with a TENCOR P-10 surface profilometer.

3. Results and discussion

Reported in this paper are the electrochemical characterization and photophysical characterization of a novel class of conjugated dendritic molecules that bear carbazoles as peripheral groups and various conjugative aromatic cores. The structures of the three molecules are illustrated in Fig. 1. The synthetic procedure used was reported in the authors' previous paper [22]. The newly synthesized materials were found to have had a good self-film-forming property and

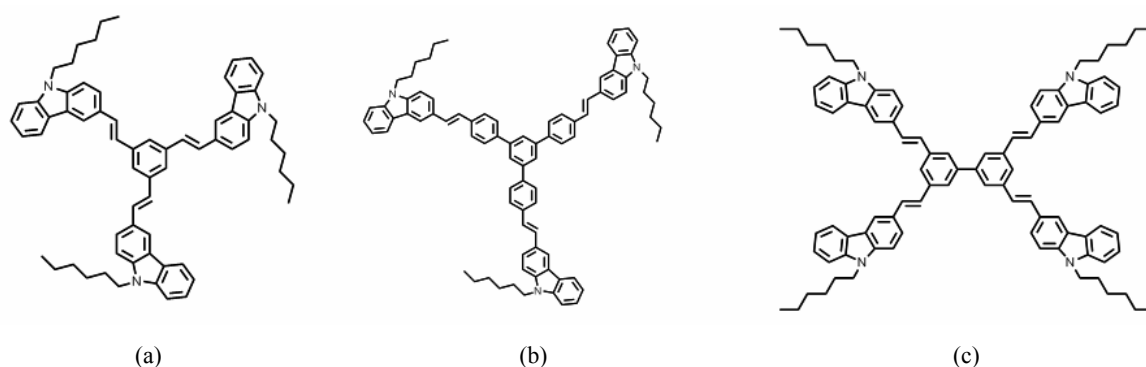


Fig. 1. Structures of the three carbazole-based dendritic molecules: (a) 3Cz, (b) 3BCz, and (c) 4BCz.

Table 1. Measured and Calculated Parameters of the Three Dendritic Molecules.

Compound	T_g ($^{\circ}\text{C}$)	T_d ($^{\circ}\text{C}$)	$\lambda_{\max}^{\text{abs.}}$ (nm)		$\lambda_{\max}^{\text{PL}}$ (nm)		HOMO (eV)	LUMO (eV)	E_g^b (eV)
			Solution ^a	Film	Solution	Film			
3Cz	50	430	346	350	417	441	-5.49	-2.50	2.99
3BCz	87	440	356	360	435	448	-5.32	-2.39	2.93
4BCz	78	450	345	349	425	437	-5.34	-2.30	3.04

^a chloroform ($c = 4 \times 10^{-6}$ M)

^b optical bandgap, E_g (eV) = $1240 / \lambda_{\text{cutoff}}$ (nm)

showed good solubility in various organic solvents such as chloroform, xylene, monochlorobenzene, and tetrahydrofuran (THF).

The thermal properties of the dendritic molecules were characterized by differential scanning calorimetry (DSC) and thermogravimetric analysis (TGA). In contrast to 3Cz, the molecules of 3BCz and 4BCz exhibited no discernible crystalline-isotropic transition up to 250°C , as observed in the DSC thermograms. (See Table 1.) This implies that they have a low degree of crystallinity and decomposition without clear melting behavior. The glass transition temperatures (T_g s) of 3Cz and 3BCz were 50 and 87°C , respectively. 3Cz has the lowest glass transition temperature due to the molecular weight effect. 4BCz did not show a clear glass transition behavior in the measuring temperature range. This indicates that 3BCz and 4BCz can exhibit an amorphous morphology in solid films, which seems useful for application to HTL or host materials in an OLED. The TGA measurements at a heating rate of $10^{\circ}\text{C}/\text{min}$ under nitrogen revealed good thermal stability. The three dendritic molecules were thermally stable up to 430 - 450°C .

Fig. 2 displays the absorption and PL spectra of the three carbazole-based compounds in the diluted chloroform solutions. The three dendritic molecules all had *meta*-

substituted carbazole moieties, and their conjugation lengths were almost identical. These resulted in the appearance of the absorption and emission maxima of all the molecules at around almost identical wavelengths. The absorption spectra in the solutions revealed characteristic carbazole absorption peaks of 346 - 358 nm. Without considering an intermolecular interaction in the diluted solution, the lower-absorption maximum wavelength of 4BCz indicates that the different geometry of the biphenyl central unit affected the oscillating strength of the conjugated bond. Generally, the red shift of λ_{\max} in a film relative to that in a solution is observed due to the intermolecular interaction between the molecules that exist in the ground state. No molecule in the film state exhibited a significant red shift in the spectrum, however, which indicates that no undesirable intermolecular interaction resulted in the isolation of the photophysical properties. (See Fig. 2 and Table 1.)

The PL spectra of the three molecules in the solutions and films were featureless and were almost a mirror-image of the low-energy absorption band. The spectral shapes indicate that the low glass transition temperature induced the various molecular conformations that diversified the energy states. Compared to the solution's spectral behaviors, in the film state, 4BCz showed a larger-absorption maximum wa-

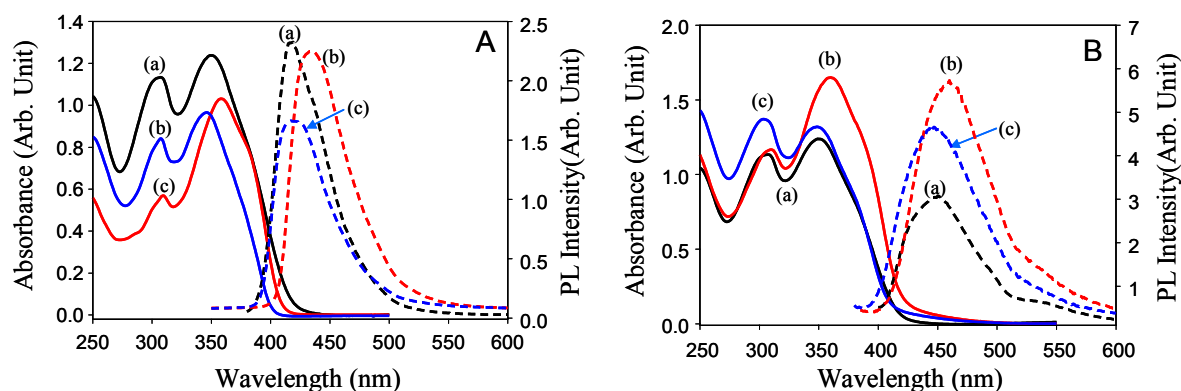


Fig. 2. Absorption and PL spectra of the carbazole-based dendritic molecules: (a) the solution in chloroform (4×10^{-6} M), and (b) the film.

Wavelength accompanied by a shoulder-like peak at 390 nm. This might have been due to the higher degree of molecular stacking through the larger core units themselves. The PL spectra of the synthesized molecules in the films exhibited a red shift of 12–24 nm and became broader in comparison to the spectra in the chloroform. These features are usually observed in organic and polymer-conjugated materials mainly due to the different polarities of their environments and their different degrees of intermolecular interaction. In particular, the PL spectra of 3Cz exhibited the largest red shift ($\Delta\lambda = 24$ nm), which indicates relatively stronger intermolecular interactions. Compared to the PL spectra in the solution states, the emission intensity at around 510–530 nm only slightly increased in the spectra of the thin films. This could be attributed to a larger extent of excimer or to intermolecular interaction. (See Fig. 2.)

The electrochemical properties of the synthesized compounds were examined via cyclic voltammetry (Model: EA161 eDAQ) to study the molecular energy levels. A platinum plate was coated with the molecular thin films using chloroform as a solvent. The potentials were obtained relative to an internal ferrocene reference (Fc/Fc^+). The HOMO and LUMO levels were determined to have been in the range of -5.32 to -5.49 eV and -2.30 to -2.50 eV, respectively. (See Table 1.) Considering the suitable energy levels for the HTL in the multilayer structural EL device, these values indicate that the compounds can potentially be used as an HTL for efficient cascading-carrier transport and as an electron-blocking layer.

Electrical and Electroluminescence Properties

3Cz, 3BCz, and 4BCz were used as the emissive materials of the light-emitting diodes (LEDs) in the multilayer

devices. A poly(ethylene dioxythiophene):poly(styrene sulfonic acid) (PEDOT:PSS) thin film was deposited on indium tin oxide (ITO) as the anode for the facilitation of the hole injection, and it was coated with the synthesized materials to form the emissive layer. A thin film of 2,9-dimethyl-4,7-diphenyl-1,10-phenanthroline (BCP) with a thickness of 10 nm was subsequently vapor-deposited on the emitting layer as a hole-blocking material to confine the exciton recombination and to limit the loss of the faster moving holes to the cathode. This was followed by the sequential deposition of a 40-nm electron injection layer of a tris(8-hydroxyquinoline) aluminium (Alq_3) and LiF (1 nm)/Al (100 nm) electrode. The EL devices with BCP/ Alq_3 layers were found to have been much more efficient than those without these layers.

The current density-voltage and luminance-voltage curves of the three dendritic molecules are shown in Fig. 3.

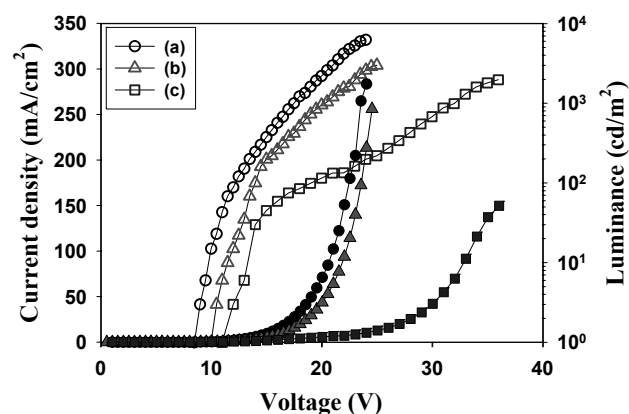
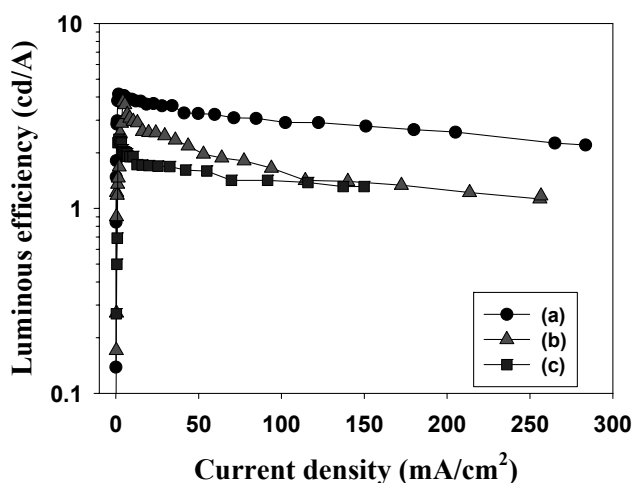


Fig. 3. Dependence of current density and luminance on the applied voltage for the following samples: 3Cz (Device A, circle); 3BCz (Device B, triangle); and 4BCz (Device C, square). Open symbol: luminance; filled symbol: current density.

Table 2. Measured Parameters of the Three EL Devices.

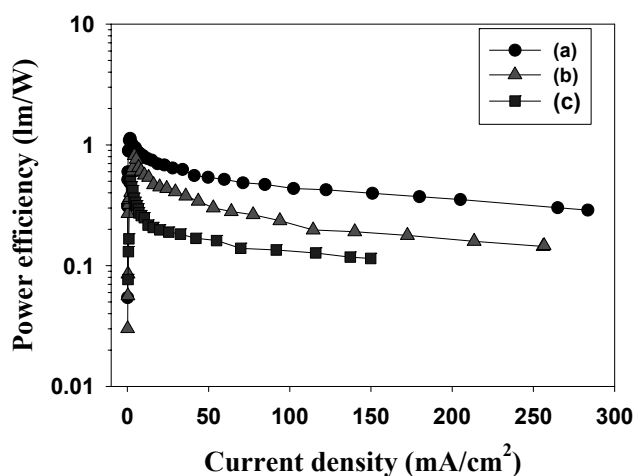
Device	Turn-on (V)	Maximum luminance/cd m ⁻² (corresponding <i>J</i>)	Maximum power efficiency/lmW ⁻¹ (corresponding <i>J</i>)	Maximum luminous efficiency/cd A ⁻¹ (corresponding <i>J</i>)	CIE Index (x, y) @500cd/m ²
Device A	8.5	6250 (283.50) at 24V	1.13(1.63) at 11.5V	4.15(1.63) at 11.5V	0.17, 0.21
Device B	10	3000 (256.64) at 25V	0.81 (4.24) at 14.5V	3.76 (4.24) at 14.5V	0.27, 0.39
Device C	11	1970 (149.85) at 36V	0.49 (1.90) at 15V	2.36 (1.90) at 15V	0.31, 0.47

**Fig. 4.** Dependence of luminous efficiency on current density for the following samples: (a) Device A, (b) Device B, and (c) Device C.

The turn-on voltages (electric fields) of the three LEDs were in the range of 8.5-11.0 V (0.7-0.8 MV/cm). The device with 3Cz showed a slightly lower turn-on voltage of approximately 8.5 V (0.5 MV/cm). The maximum brightness of the LEDs was 6,250 cd/m² at 283.5 mA/cm² (24 V) for the 3Cz device; 3,000 cd/m² at 256.64 mA/cm² (25 V) for the 3BCz device; and 1,970 cd/m² at 149.85 mA/cm² (36 V) for the 4BCz device. (See Table 2.)

Fig. 4 displays the dependence of the luminous efficiency on the current density in the three EL devices. The maximum luminous efficiencies of devices A (3Cz), B (3BCz), and C (4BCz) were 4.15 cd/A (at 1.63 mA/cm²), 3.76 cd/A (at 4.24 mA/cm²), and 2.36 cd/A (at 1.90 mA/cm²), respectively.

The maximum power efficiencies of the EL devices made of A, B, and C were 1.13 lm/W (at 1.63 mA/cm²), 0.81 lm/W (at 4.24 mA/cm²), and 0.49 lm/W (at 1.90

**Fig. 5.** Dependence of power efficiency on current density for the following samples: (a) device A, (b) device B, and (c) device C.

mA/cm²), respectively. (See Fig. 5.) It should be noted that the devices made of 3Cz showed higher luminance and efficiencies than the other devices. In a higher electric field at a higher current density, a quenching effect was highly induced in the normal multilayer EL devices. The fabricated devices showed relatively high efficiency stability, however, except for Device C, with 4BCz. The carriers were usually recombined at the emitting layer than at the interface between the hole and the electron-transporting layers. Device A exhibited an increment of the electron injection efficiency at the emitting layer and of the electron conduction within its layer.

The EL emission spectra of the devices at a constant luminance and their CIE coordinate chart are shown in Fig. 5. The three EL spectra became featureless, and particularly, Device A with 3Cz showed a significantly blue-emitting spectral behavior. Devices B and C, however, showed dif-

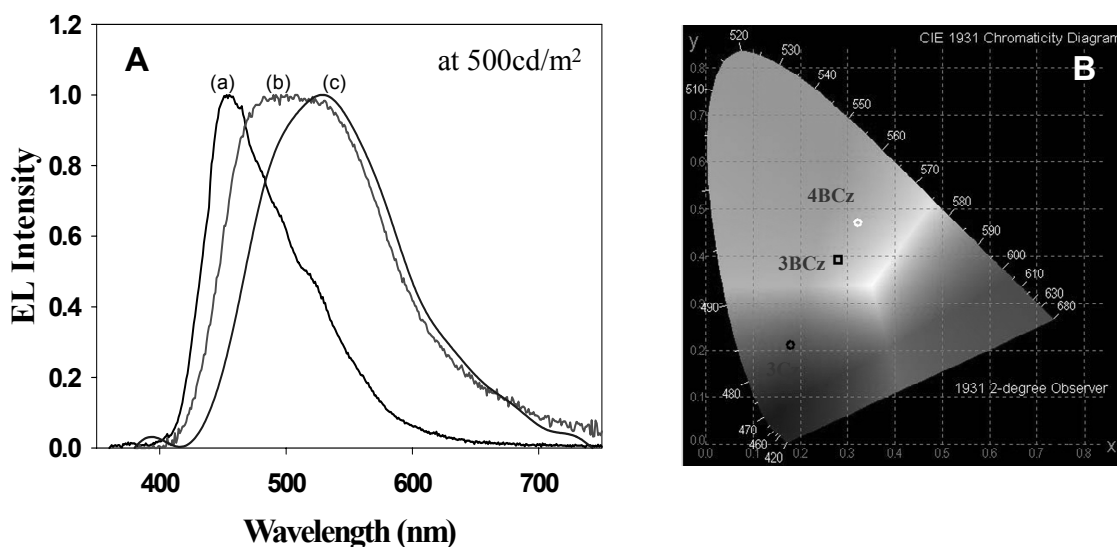


Fig. 6. (A) Electroluminescence spectra of the three devices, and (B) CIE coordinate chart of the three devices: (a) Device A, (b) Device B, and (c) Device C.

ferent spectral behaviors. They displayed greenish emissions, as can be seen in the CIE chart. To explain this, it may be conjectured that different excited-state species are responsible and superimposed for the PL and EL emissions. The larger FWHMs in the spectra of Devices B and C were possibly due to a higher degree of interactive exciton coupling in the devices. In particular, Device C showed a green emission, which might have been due to the exciplex formation between the emitting layer and the BCP. In the case of Device A with 3Cz, the EL spectrum was similar to the PL spectra, which suggests that the same excited-state species was responsible for both the PL and EL emissions. Without severe leakage of holes into the BCP and Alq₃ layers, the green emission in Device A diminished. The BCP was also crucial in the confinement of the charge recombination in the emissive layer of 3Cz and in its prevention from undesired emissions from Alq₃.

When the EL spectrum was converted into chromaticity coordinates on the CIE 1931 diagram, it was observed that the coordinates of the materials illustrated green and blue emissions, although similar carbazolyl fluorophores were used. A blue emission from 10 was obtained ($x = 0.17$, $y = 0.21$) that was different from the others, although it was not consistent with the National Television System Committee (NTSC) standard for blue color ($x = 0.14$, $y = 0.08$). [See Fig. 5 (B)]. The coordinates of Device B, which displayed greenish-white emissions, were $x = 0.27$ and $y =$

0.39. Device C with 4BCz, however, showed a green emission ($x = 0.31$ and $y = 0.47$).

4. Conclusion

Novel dendritic molecules were prepared for the emission of species in multilayer EL devices. The HOMO and LUMO energies of the synthesized molecules were found to be suitable as hole transporting materials in a multilayer EL device. The absorption and PL spectra indicated that the molecules that bore carbazoles as peripheral groups could exhibit highly isolated photophysical properties. It was also observed that the light emission of the LED devices fabricated with Device A with 3Cz was mainly from the components that contained a large-bandgap structural material, i.e., the blue emitting material. This was attributed to the prevention of exciton migration and trapping from the core moieties.

This study unambiguously demonstrated the complete utilization and future potential of dendritic molecules, which take advantage of limited exciton migration and trapping for the fabrication of better EL devices.

References

- [1] R. H. Friend, R. W. Gymer, A. B. Holmes, J. H. Burroughes, R. N. Marks, C. Taliani, D. D. Bradley, D. A. Dos Santos, J.

- L. Brédas, M. Lögdlund, and W. R. Salaneck. *Nature*, **397**, 121 (1999).
- [2] C. D. Dimitrakopoulos and P. R. L. Malenfant. *Adv. Mater.*, **14**, 99 (2002).
- [3] B. Crone, A. Dodabalapur, Y.-Y. Lin, R. W. Filas, Z. Bao, A. LaDuca, R. Sarpeshkar, H. E. Katz, and W. Li. *Nature*, **403**, 521 (2000).
- [4] C. Adachi, M. A. Baldo, and S. R. Forrest. *J. Appl. Phys.*, **87**, 8049 (2000).
- [5] Z. Hong, C. Liang, R. Li, W. Li, D. Zhao, D. Fan, D. Wang, B. Chu, F. Zang, L. S. Hong, and S. T. Lee. *Adv. Mater.*, **13**, 1241 (2001).
- [6] P. P. Sun, J.-P. Duan, H. T. Shih, and C. H. Cheng. *Appl. Phys. Lett.*, **81**, 792 (2002).
- [7] F. Liang, Q. Zhou, Y. Cheng, L. Wang, D. Ma, X. Jing, and F. Wang. *Chem. Mater.*, **15**, 1935 (2003).
- [8] M. Sun, H. Xin, K. Z. Wang, Y. A. Zhang, L. P. Jin, and C. H. Huang. *Chem. Commun.*, **6**, 702 (2003).
- [9] P. P. Sun, J.-P. Duan, J. J. Lih, and C. H. Cheng. *Adv. Funct. Mater.*, **13**, 683 (2003).
- [10] Y. Shirota. *J. Mater. Chem.*, **15**, 75 (2005).
- [11] A. Kimoto, J.-S. Cho, K. Ito, D. Aoki, T. Miyake, and K. Yamamoto. *Macromol. Rapid. Commun.*, **26**, 597 (2005).
- [12] T. W. Kwon, M. M. Alam, and S. A. Jenekhe. *Chem. Mater.*, **16**, 4657 (2004).
- [13] P. Furuta, J. Brooks, M. E. Thompson, and J. M. J. Frechet. *J. Am. Chem. Soc.*, **125**, 13165 (2003).
- [14] S.-C. Lo, T. D. Anthopoulos, E. B. Namdas, P. L. Burn, and I. D. W. Samuel. *Adv. Mater.*, **17**, 1945 (2005).
- [15] Y. Kuwabara, H. Ogawa, H. Inada, N. Noma, and Y. Shirota. *Adv. Mater.*, **6**, 677 (1994).
- [16] P.-W. Wang, Y.-J. Liu, C. Devadoss, P. Bharathi, and J. S. Moore. *Adv. Mater.*, **8**, 237 (1996).
- [17] H. Yan, B. J. Scott, Q. Huang, and T. Marks. *Adv. Mater.*, **16**, 1948 (2004).
- [18] Y. H. Niu, B. Chen, S. Liu, H. Yip, J. Bardecker, A. K. Y. Jen, J. Kavitha, Y. Chi, C. F. Shu, Y. H. Tseng, and C. H. Chien. *Appl. Phys. Lett.*, **85**, 1619 (2004).
- [19] X. H. Zhang, S. H. Choi, D. H. Choi, and K. H. Ahn. *Tetrahedron Lett.*, **46**, 5273 (2005).
- [20] J. Y. Li, D. Liu, C. Ma, O. Lengyel, C. S. Lee, C. H. Tung, and S. Lee. *Adv. Mater.*, **16**, 1538 (2004).
- [21] J. Y. Li, D. Liu, Y. Li, C. S. Lee, H. L. Kwong, and S. Lee. *Chem. Mater.*, **17**, 1208 (2005).
- [22] M. J. Cho, T. W. Lee, H. S. Kim, J.-I. Jin, D. H. Choi, Y. M. Kim, and B. K. Ju. *Macromol. Res.*, **15**, 595 (2007).